INTERNATIONAL JOURNAL FOR NUMERICAL METHODS IN FLUIDS
Int. J. Numer. Meth. Fluids 2003; **42**:623–639 (DOI: 10.1002/fld.538)

A two-scale domain decomposition method for computing the flow through a porous layer limited by a perforated plate

J. Dufrêche, M. Prat*,† and P. Schmitz

Institut de Mécanique des Fluides de Toulouse, UMR CNRS-INP/UPS No. 5502, avenue du Professeur Camille Soula, 31400 Toulouse, France

SUMMARY

A two-scale domain decomposition method is developed in order to study situations where the macroscopic description of a given transport process in porous media does not represent a sufficiently good approximation near singularities (holes, wells, etc.). The method is based on a decomposition domain technique with overlapping. The governing equations at the scale of the microstructure are solved in the vicinity of the singularities whereas the volume averaged transport equations are solved at some distance of the singularities. The transfer of information from one domain to the other is performed using results of the method of volume averaging. The method is illustrated through the computation of the overall permeability of a porous layer limited by a perforated plate. As shown in the example treated, the method allows one to estimate the useful size of the microscopic region near the singularities. As illustrated in the paper, the method can lead to a considerable gain in memory requirement compared to a full direct simulation. Copyright © 2003 John Wiley & Sons, Ltd.

KEY WORDS: porous medium; Stokes flow; Darcy flow; boundary element method

1. INTRODUCTION

In this paper, we are interested in the computation of the incompressible steady flow of a Newtonian fluid through a porous layer limited by a perforated plate. This type of situation can be encountered in filtration as a result of the particle deposition at the filter or membrane surface [1–3] as well as in other applications, for example in numerous chemical engineering processes using a fixed bed of reactive or catalytic particles. Figure 1 shows a schematic illustration of the situation under study. We assume that the direction of the average flow is perpendicular to the plate and would like to determine in particular the overall permeability of the system formed by the porous layer and the perforated plate. As shown in the figure, four characteristic lengths may be distinguished, the thickness of the layer L_z, the size of the particle ℓ, the average distance between two perforations L_x and the size of the wall perforation d. Assuming Stokes flow everywhere in the fluid domain, an approximation of

* Correspondence to: M. Prat, Institut de Mécanique des Fluides de Toulouse, UMR CNRS-INP/UPS No. 5502, ave. du Professeur Camille Soula, 31400 Toulouse, France.
† E-mail: prat@imft.fr

Received November 2001
Revised 26 August 2002

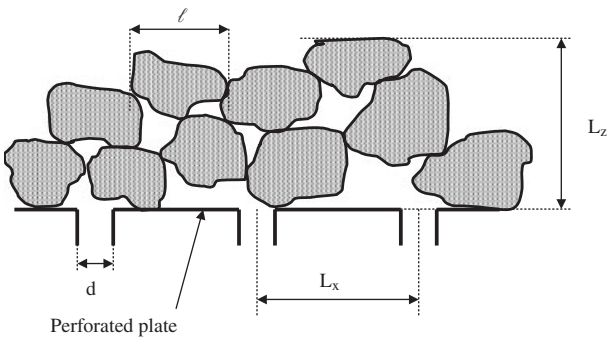

Figure 1. Schematic illustration of the situation studied.

the flow can be obtained using Darcy's law in the porous domain and appropriate boundary conditions. However, it is well known that Darcy's law is a first-order approximation of the flow which is all the better as the scale of the particle is small compared to the macroscopic scale of the porous domain (i.e. there must exist some length scale separation). In the present context, this means that we may expect reasonable predictions using Darcy's law provided L is large enough compared to ℓ, i.e. $\ell/L_z \ll 1$. However, it is clear from Figure 1 that this condition is certainly not sufficient to obtain a good approximation of the flow in the vicinity of the wall with Darcy's law if the size of the holes is not large compared to the particle size, i.e. when $d \approx \ell$. As will be illustrated in the paper, under this condition (i.e. $d \approx \ell$), the porous domain can be divided into two regions: an outer region where Darcy's law represents a sufficient approximation of the flow and an inner region, in the vicinity of the perforated wall, where the solution of the flow must be determined directly from the Stokes equations. This suggests developing a decomposition domain technique in which the flow is computed at the microscopic scale using the Stokes equations in the wall domain and at Darcy's scale in the outer domain. As the scale of description is different for the two domains, one must develop specific procedures to transfer information from one domain to the other. In the present work, these procedures have been developed using results of the volume averaging technique [4]. Although we consider a specific situation, the problem studied may be viewed as generic in the context of the continuum approach to porous medium [4, 5]. As stated above, the continuum approach results from a change in the scale of description and is associated with some length separation between the typical length scale of the macroscopic domain and the scale of the microstructure. When there exist singularities within the domain or at the boundary of the domain and when the typical length scale of the singularities (the holes in our case) is of the order of the microstructure length scales, the continuum approach may not represent a sufficient approximation and the problem must be solved directly at the scale of the microstructure in the vicinity of a singularity. For example, at a completely different scale, this is the case when transport in a fractured medium is described using a continuum model and the average distance between the fractures is of the order of a well diameter. The transport around the well must be described at the fracture scale whereas one can rely on the continuum description at some distance of the well [6]. Thus, although applied to a particular problem, the domain decomposition method presented here can be easily adapted to treat many other situations.

2. PROBLEM DEFINITION

The situation considered is shown in Figure 2. A two-dimensional spatially periodic array of cylinders is limited by a perforated plate. The distribution of perforations is spatially periodic and so one can restrict the study to a unit cell of the system. The cylinders are supposed distributed symmetrically about the axis of a perforation so that the domain of interest can be finally reduced by half. As shown in Figure 2, d is the size of perforation, ℓ the size of a unit cell of the cylinder array, L_x the distance between two perforations and L_z the thickness of the porous layer. The cylinder radius is noted R and the solid concentration C with $C = \pi R^2/\ell^2$. The full study of the overall permeability of such a system as functions of these various length scales is beyond the scope of the present paper and will be the subject of a forthcoming paper, see however Dufrêche [7]. In the present paper we focus on the two scale domain decomposition method and only consider the case where $L_z = L_x$ and $L_x/\ell = 20$. As mentioned in the introduction and made clear in the following, this method relies on the computation of the Stokes flow in the vicinity of the plate and Darcy-problem in the outer region. Typically, this implies to solve the Stokes equations over domains containing several tens of cylinders. To this end we used a spectral boundary element method (BEM) specially designed for

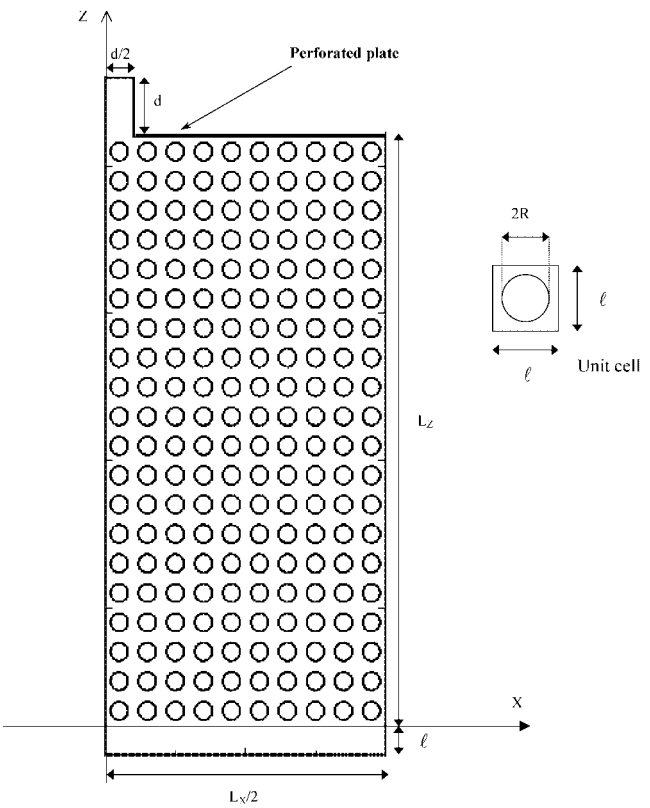

Figure 2. Two-dimensional spatially periodic array of cylinders limited by a perforated plate.

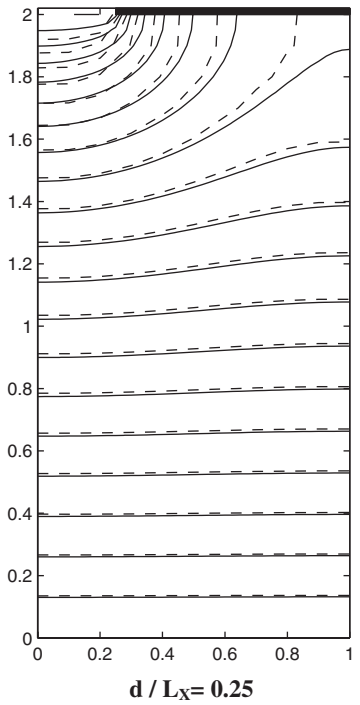

Figure 3. Isobars obtained from the Stokes problem (dashed lines) and from the Darcy problem (solid lines).

computing efficiently the Stokes flow through an array of cylinders. In particular, this BEM version leads to a considerable saving in memory size compared to a standard constant element method for results of similar accuracy. However, the particular method chosen for solving the Stokes equations is not a key issue for the two scale domain decomposition method. Any sufficiently efficient and accurate method can be used. In particular, one could also use other numerical techniques (e.g. finite element, finite difference, finite volume). For this reason, the particular BEM method we used is not presented here. Details on this method as well as a validation based on a comparison with the classic results of Sangani and Acrivos [8] can be found in Dufrêche [7]. Figure 3 shows an example of pressure field obtained solving the Stokes equation over the domain depicted in Figure 2 for the following boundary conditions:

$$\nabla \cdot \mathbf{u} = 0 \tag{1}$$

$$\mu \Delta \mathbf{u} = \nabla p \tag{2}$$

$$u_x(x) = 0, \quad u_z(x) = 1 \quad \text{at } z = -\ell \tag{3}$$

$$\text{symmetry condition at } x = 0 \text{ and } x = L_X/2 \tag{4}$$

$$u_x = u_z = 0 \quad \text{at } (d/2 < x < L_X/2, z = L_Z) \text{ and } (x = d/2, L_z < z < L_z + d) \tag{5}$$

$$u_x = u_z = 0 \text{ at the cylinder boundary} \tag{6}$$

$$u_x = 0, \quad u_z = 6U_S \frac{(\frac{d}{2} - x)(\frac{d}{2} + x)}{d^2} \quad \text{at } z = L_Z + d \tag{7}$$

where $\mathbf{u}$ is the velocity, p the (microscopic) pressure, μ the dynamic viscosity and $U_S = \frac{L_x}{d}$ the average velocity at the outlet.

As can be seen from Equation (3), a uniform velocity is imposed at the entrance of the domain. As indicated by Equation (3) and illustrated in Figure 2, the domain considered is slightly greater than the one depicted in Figure 3 in order to have a layer of free fluid of width ℓ between the first row of unit cells and the entrance of the computation domain. It may indeed be argued that it is not consistent to impose a uniform microscopic flow directly at the entrance of the first row of unit cell owing to the presence of the obstacles. Tests for various sizes of the entrance free fluid layer reveal that the perturbations due to the obstacles vanish at a distance of the order of a unit cell length, i.e. the incident frontal Stokes flow is still practically uniform at a distance ℓ away from the first row of cylinders.

As shown in Figure 2, an exit channel of length d is imposed at the exit of the system. As discussed in Dagan *et al.* [9], a channel of this length is sufficient to obtain a Poiseuille profile at the exit of the channel, consistently with Equation (7).

Figure 3 also shows the pressure field obtained using the Darcy's law, i.e. solving the following boundary value problem:

$$\mathbf{U} = -\frac{K_i}{\mu} \nabla P \tag{8}$$

$$\nabla \cdot \mathbf{U} = 0 \tag{9}$$

$$P = P_0 \quad \text{at } z = 0 \tag{10}$$

$$P = P_1 \quad \text{at } z = L_Z \ (0 < x < d/2) \tag{11}$$

$$\frac{\partial P}{\partial z} = 0 \quad \text{at } z = L_Z \ (d/2 < x < L_X/2) \tag{12}$$

$$\frac{\partial P}{\partial x} = 0 \quad \text{at } x = 0 \text{ and } x = L_X/2 \tag{13}$$

where $\mathbf{U}$ is the filtration (Darcy) velocity, P the pressure at Darcy-scale and K_i the intrinsic permeability of the cylinders array.

This problem is solved using a semi-analytic method of separation of variables [7, 10, 11].

Note that the pressure at $z = 0$ and the overall flow rate are the same in both computations (to this end the pressure field given by Equations (8)–(13) was rescaled appropriately). Also note that the location of the domain boundaries are chosen carefully in order to avoid any parasitic effects associated with the macroscopic boundary conditions. As shown in Prat [12], imposing macroscopic Dirichlet conditions (such as Equations (10) and (11)) may introduce errors of the order of $(\ell/L_z)(P_0 - P_1)$ on the pressure field computation. Here, the location of the boundaries has been chosen for this type of error to be negligible. Furthermore, note that the domain contains an integer number of unit cells. This contributes to minimize still further any error associated with the macroscopic boundary conditions. In brief, we conclude that a possible influence of the macroscopic boundary condition cannot be invoked here for

explaining the discrepancies that are observed between the overall permeability deduced from the direct computation (Stokes equations) and the one given by the Darcy model (see below). We refer the interested reader to References [12] and [13] for more details about the influence of the macroscopic boundary conditions.

Figure 3 clearly shows two main regions: a region in the vicinity of the hole where the average flow is two-dimensional and an outer region where the average flow direction is essentially perpendicular to the plate. As can be seen from Figure 3, the discrepancies between the pressure field given by the Darcy model and the one corresponding to the Stokes equations is marked in the wall region. Naturally, it may be objected that we compare here a microscopic field with a macroscopic one, i.e. fields at two different scales. However, this does not prevent us to conclude from Figure 3 that the mean pressure gradients are identical in the outer region. As the overall flow rate is the same for both computations, this indicates that the Darcy model is sufficient to predict the pressure drop in the outer region. In order to compare the overall pressure drops over the system, the overall permeability is defined as

$$K = \frac{\mu Q}{(P_0 - P_1)} \frac{L_z}{L_x} \tag{14}$$

where Q is the flow rate, P_0 the pressure at the entrance of the system and P_1 the average pressure at the exit, i.e. at $z = L_z$.

For this particular case, the overall permeability predicted with the Darcy model is $K/K_i = 0.763$ whereas the value deduced from the direct Stokes simulation is $K/K_i = 0.686$ (K_i is the intrinsic permeability of the cylinder array). Thus, the Darcy model overestimates the overall permeability compared to the direct computation based on the Stokes computation. From these results and as the mean pressure gradients are identical in the outer region, it can be concluded that the Darcy model fails in the wall region only. This is consistent with the fact that the length scale separation is not sufficient in the wall region. In other terms, the flow loses its local periodicity in the region near the hole and as a result the microscopic flow structure over a unit cell becomes sufficiently different from the spatially periodic flow structure for inducing a resistance to the flow greater than that associated with the Darcy model.

3. TWO-SCALE DOMAIN DECOMPOSITION

The above results suggest using domain decomposition ideas for computing the overall permeability. As sketched in Figure 4, the computational domain is divided into two sub-domains. The first one includes the plate. This domain is limited by the dotted line in light grey in Figure 4. The Stokes equations must be solved in this region where the problem is therefore solved at the scale of the microstructure. The second domain corresponds to the outer region where the Darcy model represents a sufficient approximation. This domain is limited by the dashed line in black in Figure 4. Note that the two domains, termed Stokes domain (Ω_S) and Darcy domain (Ω_D) in the following, overlap over a region of extension ℓ. Note also that the distance from the wall at which the overlapping region should be located is not known *a priori*. This distance depends on the accuracy which is required and must be considered as an unknown of the problem. To deal with this aspect, the procedure is to increase progressively the size of the Stokes domain until convergence of the overall permeability. Suppose now

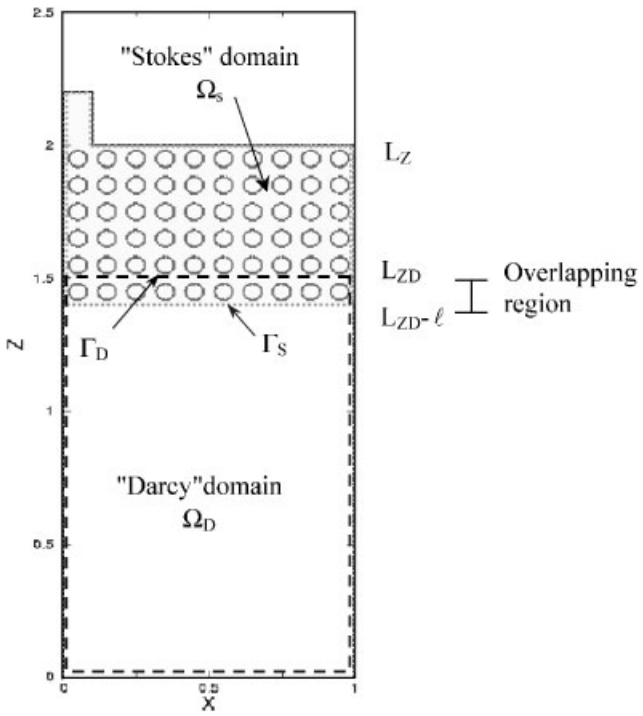

Figure 4. Schematic illustration of the two-scale domain decomposition.

that this distance is given. The computation of the overall permeability is performed using an iterative procedure that can be summarized as

(1) Compute an initial guess of the pressure field using the Darcy model in both domains.
(2) Use closure relations (Equation (15)) for determining microscopic velocities on Γ_S.
(3) Compute Stokes flow in Stokes domain using the boundary conditions on Γ_S determined in step 2.
(4) Spatially average the pressure determined in step 3 for determining macroscopic pressures on Γ_D.
(5) Compute new pressure field in Darcy domain using the spatially averaged pressure determined in step 4 as boundary condition on Γ_D.
(6) Repeat the procedure, i.e. return in (2) until convergence.

These various steps are now described in more details.

Step 1: Initial guess. An initial guess of the pressure field over Ω_D is obtained solving the Darcy problem, Equations (8)–(13), over the whole domain, i.e. $\Omega_D \cup \Omega_S$. As indicated previously, this problem is solved using a method of separation of variables [7]. Again, the particular method chosen is not a key feature of the two-scale decomposition method. A classic numerical scheme could be used as well. For this reason, the details regarding the peculiar method we used are omitted.

Step 2: Closure relations. In this step, we make use of the so-called closure relations derived within the framework of the method of volume averaging [4]. According to Barrere *et al*. [14], these closure relations can be expressed as

$$\mathbf{u} = \frac{1}{\mu}\,\mathbf{D}\cdot\nabla P \tag{15}$$

$$\tilde{p}_{\mathrm{S}} = \mathbf{d}\cdot\nabla P \tag{16}$$

D is the second-order tensor field that maps the macroscopic pressure gradient field onto the microscopic velocity field **u**. **d** is the vector field that maps the macroscopic pressure gradient field onto the microscopic spatial deviation pressure $\tilde{p}_{\mathrm{S}}$ (with $\tilde{p}_{\mathrm{S}} = p - P$). **D** and **d** must be determined numerically as explained in Appendix A for each unit cell considered, i.e. here each concentration C considered.

The closure relations lead to an accurate determination of the microscopic fields when the flow is spatially periodic at the scale of the unit cell, i.e. here when the overlapping region is located far enough from the plate for the microscopic fields to be spatially periodic. Thus, in fact, the two-scale decomposition method essentially consists in determining the distance from the singularity (i.e. here the plate) for which the microscopic flow at the scale of a representative unit cell becomes spatially periodic.

Equation (15) is used to derive the microscopic velocity field to be imposed on Γ_{S} in the next step.

Step 3: Stokes problem over Ω_{S}. The Stokes problem to be solved over Ω_{S} reads

$$\nabla\cdot\mathbf{u} = 0 \tag{17}$$

$$\mu\Delta\mathbf{u} = \nabla p \tag{18}$$

$$\text{symmetry condition at } x = 0 \text{ and } x = L_X/2 \tag{19}$$

$$u_x = u_z = 0 \quad \text{at } (d/2 < x < L_X/2, z = L_Z) \text{ and } (x = d/2, L_z < z < L_z + d) \tag{20}$$

$$u_x = u_z = 0 \text{ at the cylinder boundary} \tag{21}$$

$$u_x(x) = \frac{1}{\mu}\,(\mathbf{D}\cdot\nabla P_{\mathrm{D}}).\mathbf{i}, \quad u_z(x) = \frac{1}{\mu}\,(\mathbf{D}\nabla P_{\mathrm{D}}).\mathbf{j}, \quad \text{at } z = L_{ZD} - \ell \tag{22}$$

$$u_x = 0, \quad u_z = 6U_{\mathrm{S}}\,\frac{(\frac{d}{2} - x)(\frac{d}{2} + x)}{d^2} \text{ at } z = L_Z + d \quad \text{with } U_{\mathrm{s}} = \frac{2}{d}\int_0^{L_X/2} u_z(x, L_{ZD} - \ell)\,\mathrm{d}x \tag{23}$$

where **i** is the unit vector for the x-axis and **j** the unit vector for the z-axis. This problem is solved using the BEM technique evoked in Section 2.

Step 4: Spatial averaging. In this step a macroscopic pressure distribution on Γ_{D} is determined by spatially averaging the microscopic pressure field p determined in the preceding step. For a spatially periodic porous media, a macroscopic intrinsic variable, such as the pressure, can be defined in terms of cellular average [15],

$$P_{\mathrm{D}} = [p] = \frac{1}{V}\int_V \left[\frac{1}{V_{\mathrm{f}}}\int_{V_{\mathrm{f}}} p\,\mathrm{d}V\right]\mathrm{d}V \tag{24}$$

where V is the unit cell volume and V_{f} the volume of fluid contained within the unit cell. The cellular average is performed numerically. To this end, the values of the 'Stokes' pressure are

computed on the nodes of a discrete grid of regular spacing over each unit cell of interest. As discussed in Section 4.1, tests indicated that a grid of 14×14 points per unit cell was satisfactory for computing the above integral numerically [7]. Additional details on the cellular average are given in Appendix B.

Step 5: Darcy problem over Ω_D. The Darcy problem to be solved over Ω_D reads,

$$\frac{\partial^2 P}{\partial x^2}+\frac{\partial^2 P}{\partial z^2}=0 \tag{25}$$

$$\frac{\partial P}{\partial x}=0 \quad \text{at } x=0 \text{ and } x=L_X/2 \tag{26}$$

$$P=P_o \quad \text{at } z=0 \tag{27}$$

$$P=P_D(x) \quad \text{at } z=L_{ZD} \tag{28}$$

This problem is different from the one considered in step 1. The difference lies in the boundary condition imposed on the domain top edge (Equation (28), to be compared with Equations (11) and (12) for step 1 problem). As a result, we developed a semi-analytical method of separation of variables appropriate for this problem [7]. Again, details are omitted since other methods could be used as well.

Convergence criteria: The convergence of the procedure is estimated by computing the evolution of the boundary conditions on Γ_D and Γ_S. More precisely, we determine the evolution of the quantities C_V and C_P defined as,

$$C_V=\frac{\sum_{i=1}^{N_\Gamma}(u_x^{i_k}-u_x^{i_{k+1}})^2+(u_z^{i_k}-u_z^{i_{k+1}})^2}{\sum_{i=1}^{N_\Gamma}(u_x^{i_{k+1}})^2+(u_z^{i_{k+1}})^2} \tag{29}$$

where u_x, u_z are the components of the microscopic velocity vector (Stokes) at Γ_S. $k+1$ refers to the current iteration and k refers to the previous iteration. N_Γ is the number of nodes on Γ_S where the computation of the boundary conditions is performed.

$$C_P=\frac{\sum_{i=1}^{N_\Gamma}(P_D^{i_k}-P_D^{i_{k+1}})^2}{\sum_{i=1}^{N_\Gamma}(P_D^{i_{k+1}})^2} \tag{30}$$

where, as indicated before, $P_D=[p]$ at Γ_D. For simplicity, as indicated by Equation (30), the number of nodes considered on Γ_D is the same as on Γ_S, i.e. N_Γ.

To ensure the convergence, a relaxation method is introduced. The boundary conditions on Γ_D and Γ_S computed as described in steps 2 and 4 are corrected according to expressions of the form,

$$\chi^{k+1}=\omega\hat{\chi}^{k+1}+(1-\omega)\chi^k \tag{31}$$

with χ^k is the solution (i.e. $\mathbf{u}$ or P_D) computed for iteration k, $\hat{\chi}^{k+1}$ the solution computed for iteration $k+1$, χ^{k+1} the final boundary condition value on Γ_D or Γ_S for iteration $k+1$ and ω the relaxation parameter.

As explained before, the various steps described above are performed for a given location of the overlapping region. Once convergence is achieved for a given location, the extension of the Stokes domain is increased. We start with a Stokes domain containing two rows of

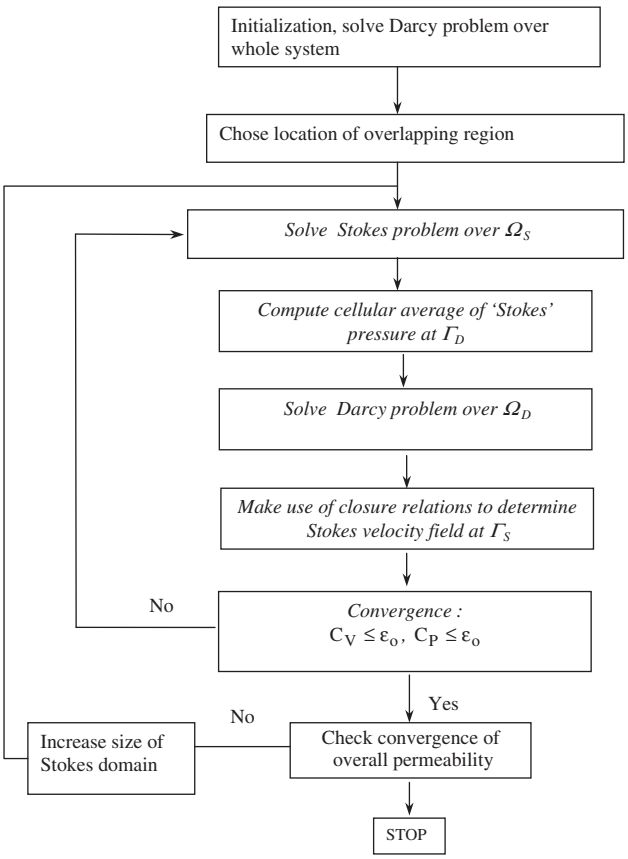

Figure 5. Chart of two-scale domain decomposition technique.

cylinders and proceed by discrete increments of size ℓ in the z-direction. Then we determine the variation of the overall permeability as a function of the position of the overlapping region. The overall permeability is finally determined when the difference between its relative value for two successive positions of the overlapping region becomes lower than a specified value, i.e.

$$\left| \frac{K_z - K_{z-\ell}}{K_z} \right| \leqslant \varepsilon$$

where K_z denotes the value of the overall permeability for Γ_S located at z. The complete procedure is summarized in Figure 5.

4. RESULTS

4.1. Validation (domain without contraction)

In this section, we consider a domain without contraction, i.e. $d = L_x$. In this case, the overall permeability is equal to the intrinsic permeability and the Darcy solution leads to an excellent

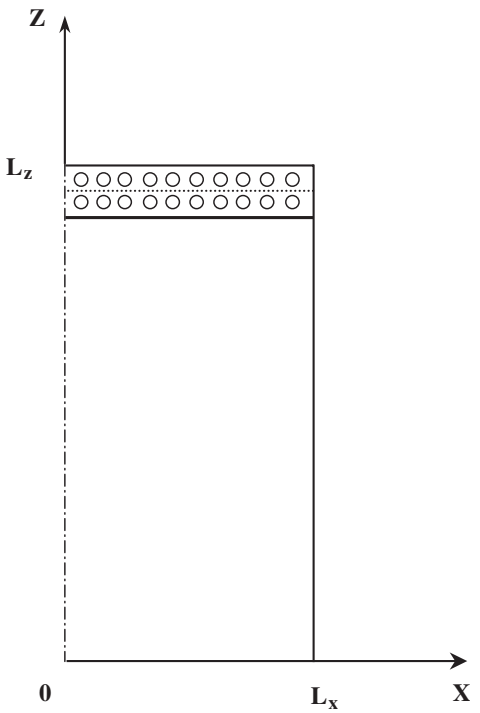

Figure 6. Computation domains for validation.

Table I. Sensitivity of the pressure cellular average to the grid size used over a unit cell (N_p is the number of grid nodes in one direction).

N_p	$[p]$	Relative error (%)
5	0.0535	7
8	0.0517	3
10	0.05054	1.08
12	0.05052	1.04
14	0.05048	0.96

estimate of the average pressure field (if care is exercised in order to avoid any parasitic effect of the macroscopic boundary conditions, as discussed in Section 2, i.e. the domain contains an integer number of unit cells). The domain considered is shown in Figure 6 with $P=0$ at $z=L_z$, $P=1$ at $z=0$ and $L_z/\ell=20$ so that $P=0.05$ at Γ_D.

We first study the influence of the number of points per unit cell necessary for performing the cellular average with a sufficient accuracy (step 4). As mentioned in Section 3, we use a grid of uniform spacing. N_p is the number of nodes per unit cell in one direction. The values of the cellular average of the 'Stokes' pressure at Γ_D are reported in Table I as a function

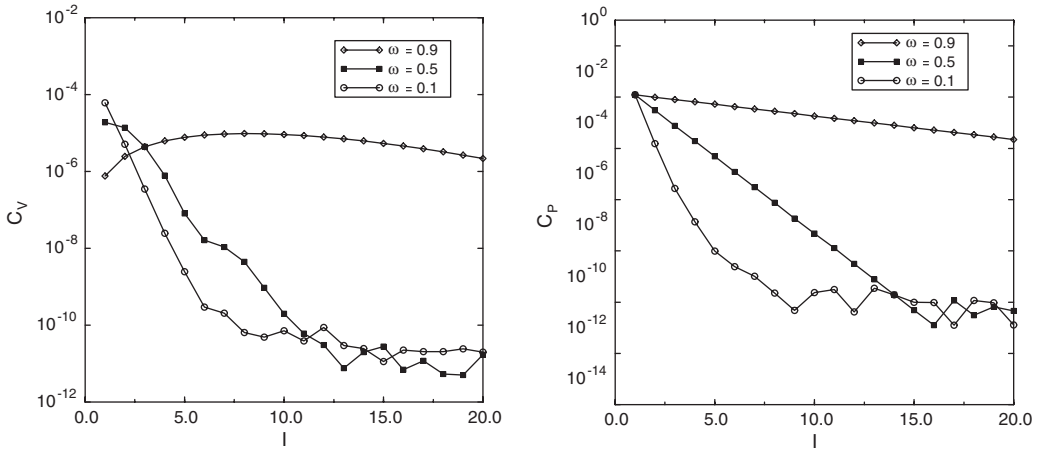

Figure 7. Evolution of C_P and C_V as a function of the number of iteration I for various values of the relaxation parameter ω (domain with no contraction).

of N_p and compared to the expected value (0.05). As can be seen from Table I, a value of $N_p = 14$ is sufficient to determine the pressure with a relative error lower than 1%. The results reported in Table I were obtained for a solid concentration of 0.3 ($C = 0.3$), i.e. the highest concentration considered in the present paper.

The influence of the relaxation parameter ω, Equation (31), is now examined. Figure 7 shows the evolution of the quantities C_V and C_P, Equations (29) and (30), as a function of the number of iterations I for three different values of ω. The results reported in Figure 7 were obtained for a solid concentration of 0.05. Similar results were obtained for higher concentrations. As can be seen from Figure 7, the smallest tested value $\omega = 0.1$ leads to the fastest convergence. This is consistent with the fact that the initial guess (Darcy solution over whole domain) is here the correct solution at the macroscopic level. Hence, this result is not general. In fact, Figure 7 merely illustrates that (1) convergence can be achieved, (2) for each situation there exist an optimum value of ω. The overall permeability deduced from the two-scale domain decomposition approach is satisfactorily found to be $K/K_i \approx 0.99$ (to be compared with the expected value (1) where K_i is the intrinsic permeability of the porous medium (K_i is determined from the solution of Stokes equation over a unit cell).

4.2. Results (domain with contraction)

We now consider a domain with contraction as depicted in Figure 4. To gain insight into the influence of the relaxation parameter ω, we consider the case with $C = 0.05$, $d/L_x = 0.1$ and $N_z = 3$ (where N_z is the size of the Stokes domain in the z-direction in number of unit cells). Figure 8 shows the evolution of C_V and C_P as a function of the number of iterations I for five different values of ω. As can be seen from Figure 8, the optimum value among the tested values is $\omega = 0.25$. This value was used for performing the simulations discussed in the following. Again, this value is close to an optimum value for the peculiar problem under study. Based on our numerical tests, the value $\omega = 0.5$ can be recommended as a robust first choice in all cases.

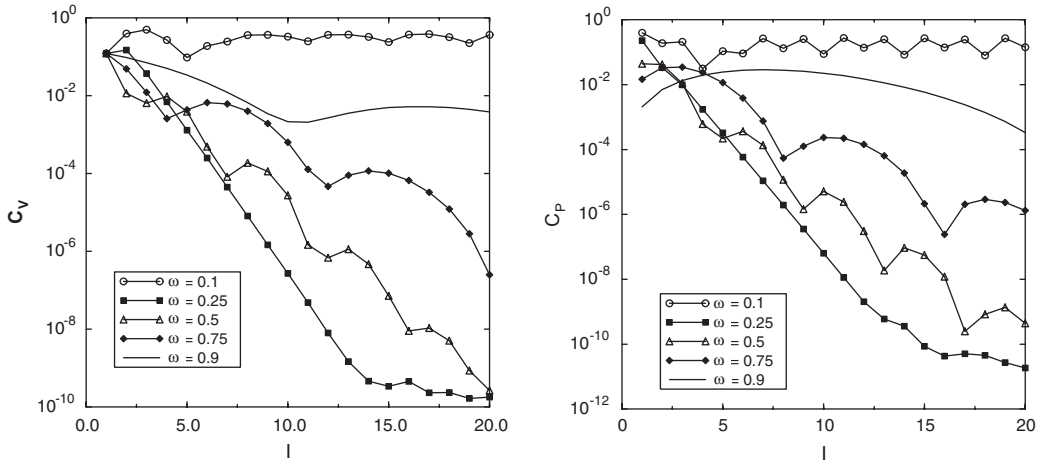

Figure 8. Evolution of C_P and C_V as a function of the number of iteration I for various values of the relaxation parameter ω (domain with contraction).

The overall permeability was computed using the two-scale domain decomposition method for various concentrations C and contraction ratio d/L_x. The most instructive cases are those corresponding to significant discrepancies between the overall permeability predicted by the Darcy model and that of the direct Stokes computation, i.e. for relatively small contraction ratios and solid concentrations. Here, we present some representative results, i.e. for $d/L_x = 0.1$ and $C = 0.05$ and 0.3. We recall that the size of the porous layer is $L_z = 20\ell$. Figure 9 shows the evolution of the overall permeability for 4 various sizes of the Stokes domain, namely $N_z = 2$, 3, 6 and 10. The case $N_z = 0$ corresponds to the Darcy solution whereas the case $N_z = 20$ corresponds to the full direct Stokes computation. As expected, the solution of the two-scale domain decomposition method converges toward the Stokes solution as the size of the Stokes domain is increased. The maximum size considered ($N_z = 10$) is still a bit too small to fully recover the Stokes solution. However, Figure 9 clearly illustrates the validity of the two-scale domain decomposition method, i.e. the microscopic description (Stokes domain here) is needed only in the vicinity of the plate and a macroscopic description (Darcy domain) is sufficient in the outer region. It is also interesting to note the rapid variations of the overall permeability with the small values of N_z.

4.3. Cost of computation and memory requirement

Figure 10 shows the evolution of the time of computation corresponding to an iteration of the two-scale domain decomposition method (i.e. a given value of N_z) as a function of the size of the Stokes domain N_z. This time is compared to the time needed for solving the Stokes problem over the full domain (for a case similar to the ones considered in Section 4.2, i.e. $L_z = 20\ell$ and $d/L_x = 0.1$). As illustrated in Figure 10, the computation time is significantly greater with the two domain approach. Therefore, the interest of the two-scale domain decomposition method does not lie in the computation cost aspect of the problem, at least for the cases investigated. As indicated in Table II, the interest lies in the gain in terms of memory storage.

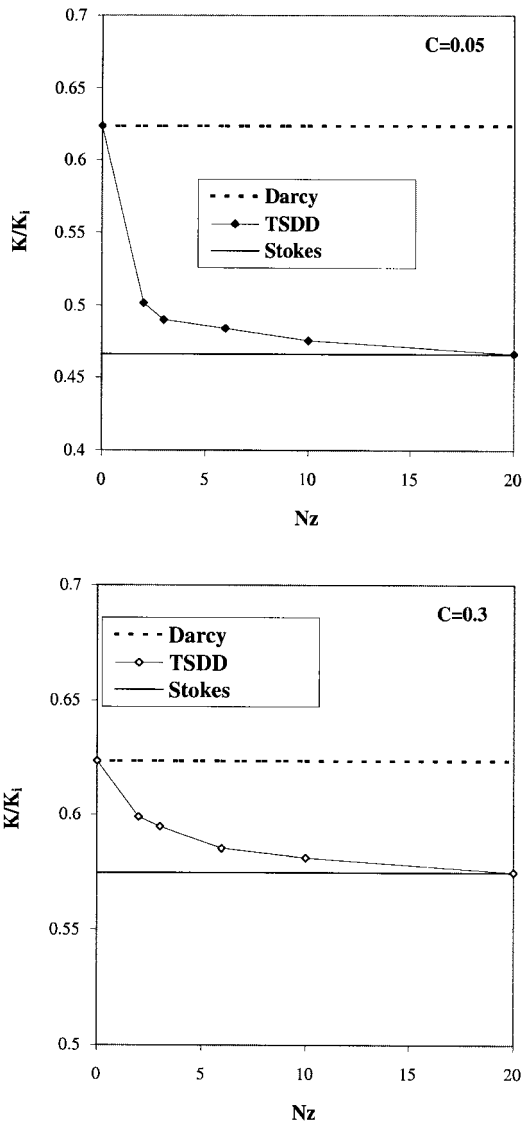

Figure 9. Evolution of the overall permeability predicted using the two-scale domain decomposition method (TSDD) as a function of the Stokes domain size N_z for $d/L_x = 0.1$ and $C = 0.05$ and 0.3. The 'Stokes' overall permeability is obtained solving the Stokes equations over the whole domain (i.e. $N_z = 20$) whereas the 'Darcy' overall permeability is obtained solving the Darcy problem over the whole domain (i.e. $N_z = 0$).

Finally, it must be emphasised again that the size of the 'microscopic' domain (Stokes domain in our example) is generally not know *a priori*. In fact, the two-scale decomposition technique can be viewed as a general method for determining the useful size of a microscopic region near a singularity.

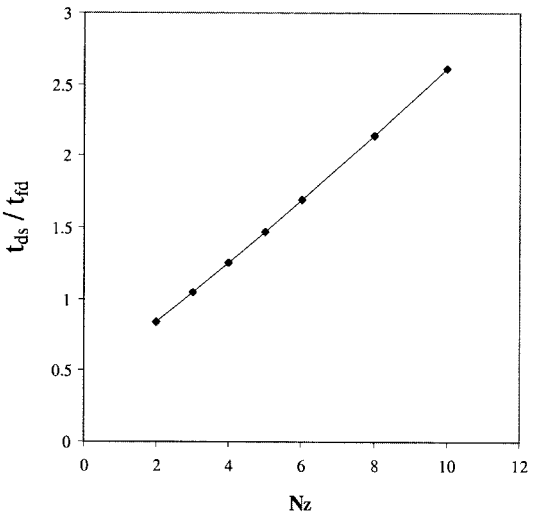

Figure 10. Evolution of the computation time t_{ts} for the two-scale decomposition method as a function of the Stokes domain size N_z. t_{fd} is the time required for the direct computation of Stokes equations over the whole domain.

Table II. Memory size requirement. Comparison between the two-scale domain decomposition (TSDD) method and the full direct Stokes computation (which corresponds to $N_z = 20$).

d/L_x	C	$\frac{\text{TSDD memory need}}{\text{'Stokes' memory need}}$	N_z
0.1	0.05	0.32	10
0.5	0.05	0.06	3
0.1	0.3	0.16	6
0.5	0.3	0.06	3

5. CONCLUSION

In this paper, a two-scale domain decomposition technique has been presented through the computation of the overall permeability of a porous layer limited by a perforated plate. This technique combines the direct computation of the governing equations at the scale of the microstructure near the plate with the computation of the average equations in the remaining part of the porous domain. The method may lead to a considerable gain in memory size compared to a full direct solution (when such a solution is possible, i.e. when the domain contains a limited number of representative elementary volumes). The gain is expected to be still much greater in three dimensions than for the two-dimensional case considered in the present paper. For the general case in which a direct microscopic simulation is completely out of reach, the method offers a constructive way of determining the useful size of the domain, near a singularity, where the problem must be solved at the microscopic level.

The method has been illustrated through a problem of single phase flow at low Reynolds number but can be implemented for many other situations and transport processes in porous

media, namely all situations and processes that can be studied within the framework of the method of volume averaging with closure problems [4].

APPENDIX A: CLOSURE RELATIONS. COMPUTATION OF TENSOR **D** AND VECTOR **d**

As shown in Reference [10], **D** and **d** are solutions of the following boundary values problem to be solved over a unit cell of the porous medium,

$$-\nabla \mathbf{d} + \nabla^2 \mathbf{D} = \mathbf{I} \quad \text{in } V_\mathrm{f} \tag{A1}$$

$$\nabla \cdot \mathbf{D} = 0 \quad \text{in } V_\mathrm{f} \tag{A2}$$

$$\mathbf{D} = 0 \text{ at the cylinder boundary (fluid/solid interface)} \tag{A3}$$

$$\mathbf{D}(x_i + \ell) = \mathbf{D}(x_i), \quad i = 1,2 \text{ at the unit cell boundary} \tag{A4}$$

$$\mathbf{d}(x_i + \ell) = \mathbf{d}(x_i), \quad i = 1,2 \text{ at the unit cell boundary} \tag{A5}$$

where **I** is the unit tensor and V_f is the fluid domain contained in the unit cell. Equations (A4) and (A5) are conditions of spatial periodicity.

In two dimensions, the above problem can be decomposed into two Stokes problems. In our case, owing to the symmetry of the unit cell, it suffices to solve only one of these two problems (see Whitaker [2] for more details). To this end, we used the BEM technique evoked in Section 2. More details can be found in Reference [5].

APPENDIX B: CELLULAR AVERAGE

For determining a macroscopic pressure from the solution of Stokes problem, we make use of a weighted average known as the cellular average, Equation (24),

$$P_\mathrm{D} = [p] = \frac{1}{V} \int_V \left[\frac{1}{V_\mathrm{f}} \int_{V_\mathrm{f}} p \, \mathrm{d}V \right] \mathrm{d}V \tag{B1}$$

where V is the unit cell volume and V_f the volume of fluid contained within the unit cell.

Within the framework of the volume averaging technique [4], the traditional average for the pressure is the intrinsic average pressure which is defined by

$$\langle p \rangle^\mathrm{f} = \frac{1}{V_\mathrm{f}} \int_{V_\mathrm{f}} p \, \mathrm{d}V \tag{B2}$$

As discussed in Whitaker [4, p. 92–93], the traditional average is the proper average for disordered system while the cellular average is the proper average for spatially periodic porous media. Proper average means an average that is devoid of small length scale (i.e. of order ℓ with our notations) fluctuations. For spatially periodic porous media, $\langle p \rangle^\mathrm{f}$ is affected by such small scale fluctuations while the cellular average, which is nothing else than a spatial average of $\langle p \rangle^\mathrm{f}$ over the unit cell volume ($[p] = (1/V) \int_V \langle p \rangle^\mathrm{f} \, \mathrm{d}V$), is not. On can refer to Whitaker [4] or Quintard and Whitaker [15] and references therein for mode details.

ACKNOWLEDGEMENTS

We are grateful to Dr J.M. Frey for many useful discussions, suggestions and developments regarding some of the numerical methods used in this work.

REFERENCES

1. Elimelech M, Gregory J, Jia X, Williams R. *Particle Deposition & Aggregation*. Butterworth-Heinemann: Oxford, 1995.
2. Schmitz P, Wandelt B, Houi D, Hildenbrand M. Description of particle aggregation at the membrane surface in crossflow microfiltration. *Journal of Membrane Science* 1993; **84**:171–183.
3. Frey JM, Schmitz P. Particle transport and capture at the membrane surface under cross-flow microfiltration. *Chemical Engineering Science* 2000;**55**:4053–4065.
4. Whitaker S. *The Method of Volume Averaging*. Kluwer Academics Publishers: Dordrecht, 1999.
5. Bear J, Bachmat Y. *Introduction to Modeling of Transport Phenomena in Porous Media*. Kluwer Academics Publishers: Dordrecht, 1990.
6. Quintard M. Private communication.
7. Dufrêche J. Ecoulement à travers une couche poreuse limitée par une paroi perforée: comparaison entre approche de Darcy et simulations numériques à l'échelle microscopique. *Ph.D thesis*, INPT, France, 2000.
8. Sangani AS, Acrivos A. Slow flow past periodic arrays of cylinders with application to heat transfer. *International Journal of Multiphase Flow* 1982; **8**:193–206.
9. Dagan Z, Weinbaum S, Pfeffer S. An infinite-series solution for the creeping motion through an orifice of finite length. *Journal of Fluid Mechanics* 1982; **115**:505–523.
10. Poulikakos D. *Conduction Heat Transfer*. Prentice-Hall: Englewood Cliffs, NJ, 1994.
11. Gustafson KE. *Partial Differential Equations and Hilbert Space Methods*. Wiley: New York, 1980.
12. Prat M. On the boundary conditions at the macroscopic level. *Transport in Porous Media* 1989; **4**:259–280.
13. Prat M. Some refinements concerning the boundary conditions at the macroscopic level. *Transport in Porous Media* 1992; **7**:147–161.
14. Barrère J, Gipouloux O, Whitaker S. On the closure problem for Darcy's law. *Transport in Porous Media* 1992; **7**:209–222.
15. Quintard M, Whitaker S. Transport in ordered and disordered porous media: volume-averaged equations, closure problems, and comparison with experiments. *Chemical Engineering Science* 1993; **48**(14):2537–2564.

